

## MEASUREMENTS OF Nb<sub>3</sub>Sn CONDUCTOR DIMENSION CHANGES DURING HEAT TREATMENT

D. Bocian, G. Ambrosio, G. M. Whitson

Fermi National Accelerator Laboratory  
P.O. Box 500, Batavia, IL 60510-0500, USA

### ABSTRACT

During the heat treatment of Nb<sub>3</sub>Sn coils the conductor material properties change significantly. These effects together with the changes of the conductor dimensions during heat treatment may introduce large strain in the coils for accelerator magnets.

The US LHC Accelerator Research Program (LARP) has initiated a study aiming at understanding the thermal expansion and contraction of Nb<sub>3</sub>Sn strands, cables and coils during heat treatment. Several measurements on strands and cables were performed in order to have sufficient inputs for finite element simulation of the dimensional changes during heat treatment. In this paper the results of measurements of OST-RRP Nb<sub>3</sub>Sn conductor used in the LARP magnet program are discussed.

**KEYWORDS:** Accelerator magnets, superconducting magnets, superconducting wires, heat treatment, mechanical properties

### INTRODUCTION

The US LHC Accelerator Research Program (LARP) has a primary goal to develop, assemble and test Nb<sub>3</sub>Sn quadrupole magnet models for a luminosity upgrade of the Large Hadron Collider (LHC) [1-3]. In order to produce magnets with high field uniformity a precise placement of the coil windings is required. Movement of the conductor and other components during coil heat treatment (HT) can alter magnet design from the ideal configuration.

The strain state of the conductor is a critical parameter for the fabrication of Nb<sub>3</sub>Sn superconducting coils. During the heat treatment several intermetallic phases develop in the conductor before Nb<sub>3</sub>Sn formation. The changes of material properties and the interaction with pole parts and heat treatment fixtures may introduce significant strain in the coil.

The highest critical current densities in long length (production) Nb<sub>3</sub>Sn strands, with high reproducibility, are presently achieved through the Restacked Rod Process (RRP) by

Oxford Instruments – Superconducting Technology (OST) in the USA [4]. RRP strands, presently the only conductor used by the LARP collaboration, are the subject of this study.

The objective of the study presented in this paper is to characterize dimensional changes and to prepare data for finite element modeling (FEM) of the thermal expansion and contraction of RRP Nb<sub>3</sub>Sn strands, cables and coils during the heat treatment. Several intermediate step studies have been completed including the review and collection of relevant data in literature as well as discussion with experts in order to identify the critical steps of this analysis. Only a limited set of data was found relevant to the planned analysis[5-7], and most data were collected for significantly shorter HT reaction durations. It was also noticed that the number of measured samples was insufficient from a statistical point of view. This fact motivated us to prepare and perform a series of measurements of strands used in LARP magnet program. The measurements of strand length change, strand radial increase and also strand twist change of unconstrained strand samples after heat treatment were performed. Since we observed some disagreement with published results [6] the measurements were carefully repeated and analyzed in order to answer all possible questions.

In the first paragraph of this paper the reaction process, optimized for LARP coils, is discussed. The experimental setup and results of measurements are subsequently presented. Finally results are summarized and possible future steps of this analysis are discussed.

## HEAT TREATMENT SIMULATION

The superconducting A15 phase in internal-tin Nb<sub>3</sub>Sn strands (as RRP) is produced from the ductile precursor elements Nb and Sn during a reaction heat treatment. During reaction Sn diffuse to the copper in the subelement bundle, forming various intermetallic phases and finally the superconducting Nb<sub>3</sub>Sn. The heat treatment cycles of Nb<sub>3</sub>Sn superconductor are optimized to achieve high critical current (I<sub>c</sub>) and therefore are often very long. The HT process, optimized for both high critical current and high stability current [8] in LARP magnets with 90-mm aperture [1-3, 9-10] is depicted in Figure 1. The reaction cycle was tested on strand and cable samples and short Technological Quadrupole (TQ) magnets [9-10] with the same conductor (OST RRP 54/61).

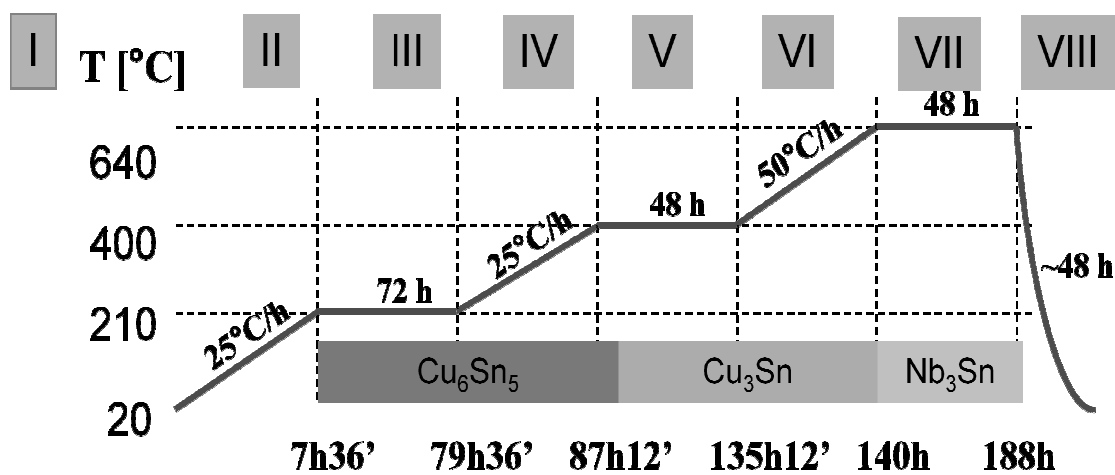


**Figure 1** Heat treatment reaction optimized for LARP 90-mm aperture Nb<sub>3</sub>Sn quadrupole coils.

In order to model the Nb<sub>3</sub>Sn reaction process the diagram depicted in Figure 1 has been divided into eight steps. For each step the elasticity modulus (E), the

density ( $\rho$ ), and the coefficient of thermal expansion (CTE) are needed. Another critical part of the simulation is phase transition modeling. The general simulation plan is presented in the following steps:

- I. Prepare and perform 3D simulation of strand with ANSYS.
- II. Validate strand model with measurement results. Adjust the model parameters.
- III. Simplify strand model and use it to build cable model.
- IV. Validate cable model with measurement results. Adjust the model parameters.
- V. Simplify cable model and use it to build coil model.
- VI. Validate coil model with measurement results. Adjust the model parameters.

## **EXPERIMENTAL SETUP**

Most strand and cable samples were heat treated together with LARP Long Quadrupole coils in a 6 m long oven at Fermilab. A few strand samples were heat treated in a small oven. During reaction, the oven temperature was monitored continuously by thermocouples placed around and within the reaction fixture. Gas tight reaction furnaces are used at Fermilab with 99.99% pure argon gas to perform the coil heat treatment. Two gas supplies are used, one for the furnace volume with a flow rate of 24 L/min (50 SCFH) and one for the reaction tooling using a gas flow rate of 12 L/min (25 SCFH). These flow rates maintain a small positive pressure within the reaction fixture and the furnace. Exhaust gas from the reaction fixture is passed through a filter to capture residues of oil (used for strand manufacturing) and of palmitic acid (a binder used to strengthen the cable insulation). Temperature uniformity within the furnace volume is maintained within  $\pm 3^\circ\text{C}$  at all three temperature plateaus. The strand samples were placed in a barrel connected in series with the reaction fixture, so they were reacted in the same atmosphere of the reacted coil.

The main goals were to measure length and diameter change during reaction, as well as strand twist change. The work was divided into several phases, namely: sample cut; sample ends preparation; precise length and diameter measurement before and after heat treatment.

### **Samples preparation**

The object of this study were RRP 54/61 and RRP 108/127 strands, made by OST, used in the LARP magnet program. The strand sample length ranged from 50 to 1000 mm. The nominal strand diameter for measurements presented in this paper was 0.7 mm for twisted RRP 54/61 and RRP 108/127 samples, and 0.85 mm for “non-twisted” RRP 108/127 samples. In all reaction campaigns only strand samples from the same billets for each type of strand were used in order to reduce variability. The samples were inserted into quartz tube to keep them straight and to reduce environment impact. Nonetheless environment impact was studied by reaction of some strand samples in larger mica tubes as well as in small and in large oven. Results show no dependence on the type of reaction tube and oven type. In order to select the correct sample ends preparation method for further measurements the impact of different ends preparation (crimped, fused and as cut) was studied. Finally samples with fused ends were chosen as default for further reactions. These types of end preparation were studied also for developing the best preparation for the samples to be measured with a dilatometer. The procedure selected (fusing the ends, and

subsequent filing) was chosen in order to protect the sample against Sn leak from the stands (Figure 2 - Figure 4) and to provide a smooth surface for the length measurement

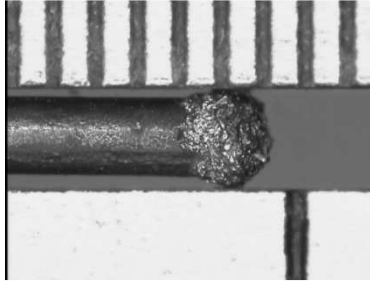


**Figure 2** Selected example of sample end after reaction. The photo shows strand end “as cut” with visible Sn leak during reaction. That is why “as cut” sample end preparation was rejected.

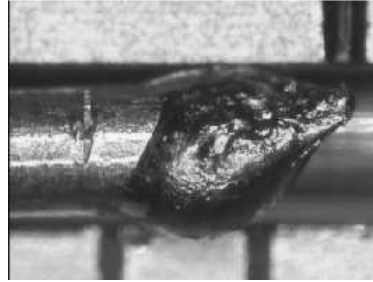


**Figure 3** Selected example of fused sample end. The photo shows that after fusing majority of the samples have not regular end shape. In order to perform precise sample measurement a fine filing is necessary.

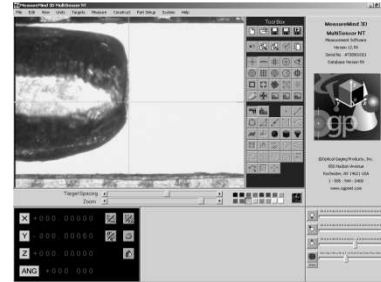


**Figure 4** Selected fused sample ends after filing. Picture shows that fine strand end preparation allows high precision measurement of sample length change.

## Samples measurement

The measurements of strand sample length were performed with ATS-800 Video Measuring System (Figure 5 and Figure 6) with total measurement precision of 5  $\mu\text{m}$ . The same measurements precision were obtained for strand diameter measurements performed with micrometer. The twist change with a dedicated tool was measured with 0.5 degree accuracy.



**Figure 5** ATS-800 Video Measuring System (VMS). This system allows measuring samples with precision of 5  $\mu\text{m}$  assuming recurrent measurements.



**Figure 6** Micro-markers on the stand surface used for fractional strand length change measurement. The markers were made with scalpel by gentle touching of strand surface in order to avoid cut of strand subelement with Sn inside (avoiding Sn leak). The width of the markers is order of 80  $\mu\text{m}$ .

## MEASUREMENT RESULTS

The following measurements, before and after heat treatment, were performed: strand diameter change, strand length change and strand twist change.

The diameter change ( $\Delta D/D$ ) measurements shown in Figure 7 were performed with OST RRP 54/61 strands. They demonstrate RRP 54/61 strand radial increase by average value of 2.15%. Each strand diameter measurement was taken 10 times over the sample length resulting in the error of the average of 0.2%. The majority of results plotted in Figure 7 are within this error range. These results are in good agreement with data published in [7], performed also with OST RRP 54/61 strands. The different marker shown



sample. The end effect is clearly shown in Figure 10 by the peaks at the ends of the samples. Since the end segments were quite short, of the order of 1.2 mm, the measurements error of the end segments is large: 0.4% of the segment length (with 5  $\mu\text{m}$  precision of measuring tool). However many samples were measured and all of them showed an increase of  $\Delta L/L$  at the ends. Therefore, with higher statistics, the error of the average decreases to about 0.1% (for 10 samples) resulting in a clear effect. Since a goal of ours is to measure a short sample with a dilatometer, we have to take into account this effect during the sample preparation and measurement.

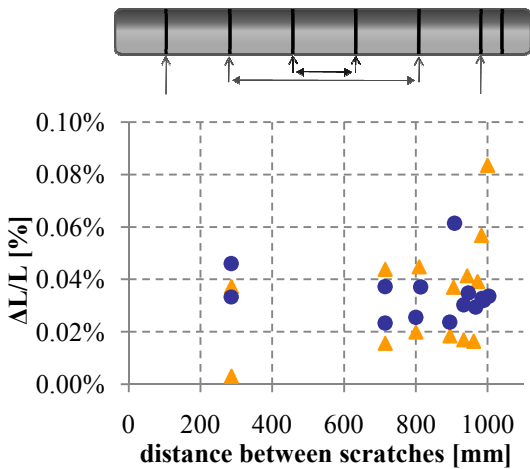


**Figure 9** OST RRP 54/61 strand fractional length change. Several micro-markers were placed on the strand surface in order to measure fractional length change. The different markers refer to different measured samples.

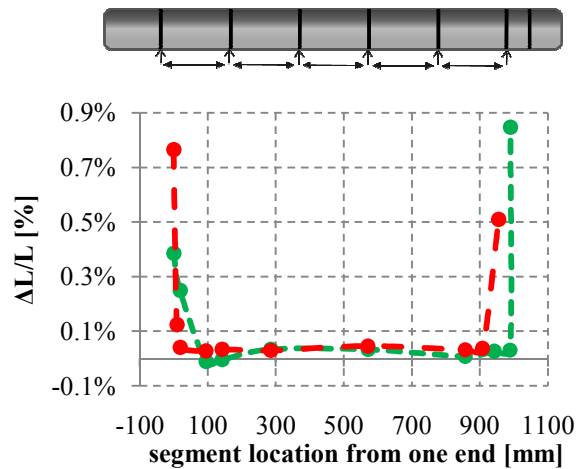


**Figure 10** OST RRP 54/61 strand fractional end change with respect to the position of the measured segment along the sample. A large end effect was observed. To clearly demonstrate end effect only two selected measurements were plotted in this figure.

Measurement of twist change and its impact on sample length are presented in Figure 11 and 12.

Since the same samples were used for diameter, length and twist change study, the measurements of twist change over the sample length presented in Figure 11 were performed with RRP 54/61 strand type. No significant dependence on sample length or position can be observed. All results are within the error range. The average twist change of RRP 54/61 is 1.6 deg/mm. Also measurements of twist change for RRP 108/127 have shown the twist change of 1.3 deg/mm (see: TABLE 1).

In order to measure strand twist change impact on  $\Delta L/L$  two types of strands, twisted and “non-twisted”, from the same billet, were reacted and measured. This study was performed with OST RRP 108/127 strands since “non-twisted” RRP 54/61 strands samples were not available. A precise measurement of twist change shows that also “non-twisted” samples during production process were a little twisted (average 0.4 deg/mm) but it is factor 70 less than twisted samples (in average 28 deg/mm for both RRP 54/61 and RRP 108/127).

Figure 12 shows the results of twist change impact on sample length change. Round markers show average results over the sample length for twisted RRP 108/127,  $d=0.7$  mm samples and diamond show average results for “non-twisted” RRP 108/127,  $d=0.85$  mm samples. Both strand samples are from the same billet (#12521). The nominal diameter difference comes from the production procedure. Strand is twisted and drawn in the last turn, reducing strand size from 0.85 to 0.7 mm. The results shown in Figure 12 confirm that strand twist change (“untwist”) contributes to the strand elongation.

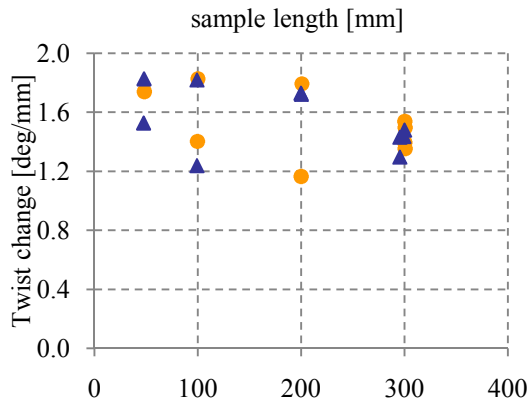


**Figure 11** OST RRP 54/61 strand twist change. The different markers refer to different measured samples.

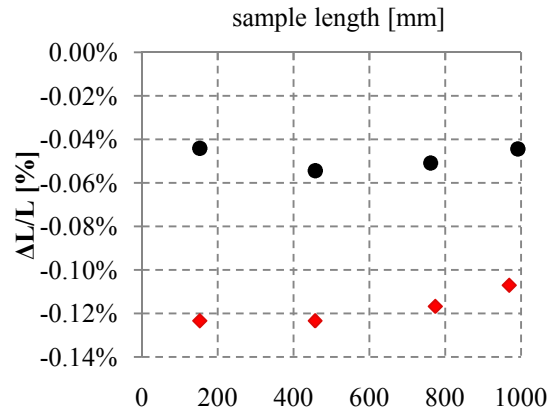


**Figure 12** Impact of the strand twist on sample elongation. Round markers show results of twisted samples and diamond results of non-twisted sample

TABLE 1 summarizes the results of measurements performed with different types of strands. It shows that OST RRP 54/61 strands elongate whereas OST RRP 108/127 strands shrink after heat treatment (although by small amount in both cases). “Non-twisted” RRP 108/127 strands shrink significantly more than the same strands when twisted. The diameter change show correlation with Copper to superconductor ratio (RRP 54/61: Cu/sc = 0.85, RRP 108/127: Cu/sc = 1.155). Length and diameter changes in the table are shown together with the ranges of maximal and minimal measured results.

**TABLE 1** Results of Nb<sub>3</sub>Sn strands and cables measurements. The errors shown for length and diameter measurements show the spread of measured data.

SAMPLE	Length change [%]	Diameter change [%]	Twist change [deg/mm]
STRAND RRP 108/127 (billet 12521, twisted)	-0.045 <sup>+0.025</sup> <sub>-0.015</sub>	+1.88 <sup>+0.07</sup> <sub>-0.04</sub>	-1.3 <sup>*</sup>
STRAND RRP 108/127 (billet 12521, non-twisted)	-0.12 <sup>+0.02</sup> <sub>-0.03</sub>	+1.71 <sup>+0.06</sup> <sub>-0.05</sub>	-0.26 <sup>**</sup>
STRAND RRP 54/61 (billet 9532, twisted)	+0.035 <sup>+0.025</sup> <sub>-0.035</sub>	+2.15 <sup>+0.7</sup> <sub>-0.25</sub>	-1.6 <sup>*</sup>

\* nominal twist is 28 deg/mm

\*\* nominal twist is 0.4 deg/mm

## CONCLUSIONS AND FUTURE PLANS

A study of OST RRP Nb<sub>3</sub>Sn strands behavior during heat treatment was presented. Several measurements before and after HT were performed and compared in order to understand the strand dimensional changes during the heat treatment.

The results show that unconstrained twisted strands untwist during the heat treatment by about 4%. The untwisting causes the elongation not present in untwisted strands made from the same billet. In Rutherford cable the strands are constrained by the layout of the cable, therefore we suggest measuring untwisted strands in order to predict the length change during HT of Rutherford cables and coils.

This study also showed that the ends of the strand samples, fused to prevent tin leaks during the HT, have a larger relative elongation during the HT. This end effect should be taken into account when measuring short samples to predict the length change of longer strands, cables or coils.

The measurement of diameter change of 1.9% and 2.15% for twisted RRP 108/127 and RRP 54/61 strands respectively, confirmed the expected dependence on the copper to superconductor ratio.

Presently on-line measurements of length change during the HT are in progress with a dilatometer at the NHMFL in Tallahassee (FL) on samples made by seven strands fused together. The short length of the samples will require a detailed analysis in order to extract the behavior of the central section by removing the end effects.

## ACKNOWLEDGEMENTS

The main author would like to thank E. Barzi, T. Beale, D.R. Dietderich, M. Field, A. Ghosh, A. McInturff, A. Nobrega, J. Parrell, D. Turrioni for their help and support during the course of this work.

This work was supported by Fermi Research Alliance, LLC, under contract No. DE-AC02-07CH11359 with the U.S. Department of Energy; by the Director, Office of Science, High Energy Physics, U.S. Department of Energy under contract No. DE-AC02-05CH11231, and partially supported by the DOE through the US LHC Accelerator Research Program (LARP).

## REFERENCES

1. G. Ambrosio, et al., "Design of Nb<sub>3</sub>Sn coils for LARP long magnets", *IEEE Trans. on Appl. Supercond.*, vol. 17, no. 2, pp. 1035-1038, 2007
2. G. Ambrosio, et al., "Development and Coil Fabrication for the LARP 3.7-m Long Nb<sub>3</sub>Sn Quadrupole", *IEEE Trans. on Appl. Supercond.*, vol. 19, 2009
3. G. Ambrosio, et al., "LARP Long Nb<sub>3</sub>Sn Quadrupole Design", *IEEE Trans. on Appl. Supercond.*, vol. 18, no. 2, pp. 268 - 272, 2008;
4. J. A. Parrell *et al.*, "High field Nb<sub>3</sub>Sn conductor development at oxford superconducting technology", *IEEE Trans. on Appl. Supercond.*, vol. 13, no. 2, pp. 3470-3473, 2003
5. Dietderich D.R. *et al.*, "Dimensional changes of Nb<sub>3</sub>Sn, Nb<sub>3</sub>Al, and Bi<sub>2</sub>Sr<sub>2</sub>CaCu<sub>2</sub>O<sub>8</sub> conductors during heat treatment and their implication for coil design." *Adv. Cryo. Eng.*, vol. 44b, pp. 1013–1020
6. Scheuerlein Ch. *et al.*, "Phase Transformations During the Reaction Heat Treatment of Internal Tin Nb<sub>3</sub>Sn Strands With High Sn Content", *IEEE Trans. on Appl. Supercond.*, Vol.18, No. 4, 2008;
7. Andreev N. *et al.*, "Volume expansion of Nb-Sn strands and cables during heat treatment", *Adv. in Cryogenic Eng.*, vol. 48B, p.941, 2001
8. Barzi E. *et al.*, "RRP Nb<sub>3</sub>Sn Strand Studies for LARP", *IEEE Trans. on Appl. Supercond.*, vol. 17, no. 2, pp. 2607-2610, 2007;
9. S. Feher *et al.*, "Development of LARP Technological Quadrupole (TQC) Magnets", *IEEE Trans. on Appl. Supercond.*, vol. 17, no. 2, pp. 1126-1129, 2007;
10. S. Caspi *et al.*, "Fabrication and Test of TQS01—A 90 mm Nb<sub>3</sub>Sn Quadrupole Magnet for LARP", *IEEE Trans. on Appl. Supercond.*, vol. 17, no. 2, pp. 1122-1126, 2007;